An improved assessment of high efficiency heterojunction perovskite solar cell employing $In_xGa_{1-x}As$ as efficient hole transport layer

Mohammed Khaouani (m.khaouani@univ-chlef.dz)
Hassiba Benbouali University of Chlef: Universite Hassiba Benbouali de Chlef https://orcid.org/0000-0001-8025-0621

H. Bencherif
University of Batna 2: Universite Batna 2

kourdi zakarya
Algerian Space Agency: Agence Spatiale Algerienne

Research Article

Keywords: Heterojunction perovskite solar cell, InGaAs, HTM, numerical simulation

Posted Date: January 31st, 2022

DOI: https://doi.org/10.21203/rs.3.rs-1231901/v1

Abstract

Spiro-OMeTAD is an excellent nominee for HTM application, but its high hygrpscopicity, inclination to crystallize, and fragility to moisture and heat make it unsuitable for solar cells. So, it is of interest to investigate other HTM candidate. In this paper, the use of p-type InGaAs as hole transport materials (HTM) has been suggested to enhance the performance of perovskite-based solar cell (PSC). The simulation of hybrid CH3NH3PbI3/ InGaAs planar heterojunction perovskite solar cell is performed using Atlas Silvaco simulator. In order to confirm the predictability of the proposed simulation methodology, the conventional ITO/TiO_2/$MAPbI_3$/Spiro-OMeTAD structure is simulated and good coincidence with experimental results shown. The proposed design using InGaAs as HTM outperforms the conventional device in terms of short-circuit current density (J_{SC}) of 37.2 mA/cm2, open-circuit voltage (V_{OC}) of 1V, fill factor (*FF*) of 80% and high value of efficiency. Besides, The finding show that with In content of x=0.7 the efficiency will improved to reach a value of about 30%.

I. Introduction

In past years, the optical and electrical characteristics of the hybrid organic/inorganic methylammonium lead iodide CH3NH3PbI3 perovskite solar cell (PSC) have been intensively explored [1]. The PSC ought to be capable of competing with traditional silicon-based solar cells due to its low cost and simple manufacture technique. The mesoporous structure [2] and the planar heterojunction structure [3] have both affected the development of the PSC. Electron transport material (ETM)/absorber/hole transport material (HTM) are the three major layers of electron transport material in conventional planar PSC [4]. TiO2 and spiro-OMeTAD are the most extensively utilized ETM and HTM, respectively. The time-consuming synthesis of spiro-OMeTAD, on the other hand, represents an impediment to future commercialization due to its high cost [5]. Furthermore, it is well recognized that spiro-OMETAD degrades PSC efficiency. For example, a PSC that used Spiro-OMeTAD as the HTM of the PCE for just three months saw a 22 percent reduction in 500 hours of 45°C light [6], and a 20 percent reduction in 500 hours of 45°C light [7]. As a result, new types of HTM must be sought. CuI [8], CuSCN [9], Cu2O [10], NiO [11], and V2O5 [12] are examples of inorganic p-type materials that can be used as HTM to minimize the cost of the PSC while also improving its stability. To minimise carrier recombination, the search for a suitable inorganic HTM must be directed by the necessity for high carrier mobility, low cost, and a defect-free interface with the absorbing layer [13]. In comparison to spiro-OMeTAD, an optimal type of HTM is inorganic p-type InGaAs, which has superior chemical stability, increased hole mobility, and cheap cost [14]. As a result, p-InGaAs as HTM is an unique perovskite solar cell concept.

The excellent absorber p-InGaAs will result in generation of photocurrent in the p-InGaAs perovskite solar cell. Perovskite, on the other hand, has higher optical absorption characteristics than P-InGaAs. We designed the CH3NH3PbI3/p-InGaAs planar heterojunction perovskite solar cell based on the good features of perovskite and p-InGaAs. As a new PSC, the perovskite/p-InGaAs heterojunction perovskite solar cell, it is vital to analyse the influence of the PSC's operation mechanism in order to obtain high performance. Many details like the band offset, in mole fraction, optimum thickness, and optical

performance of the p-InGaAs perovskite solar cell, however, ought to be examined. The simulation can lead to a new way of thinking about how to make PSC structures that are simpler and more efficient. Device simulation is performed in this paper to analyze the suggested structure's efficiency, which results in high electrical outputs. High J_{SC} and V_{OC} of are gained. The efficiency attains a 30% for In content of 0.7%.

Ii. Devices Structure

Figure 1 shows the conventional and the proposed solar cell using InGaAs as HTM. It comprises of a transparent contact (ITO), a n type ETL material (TiO_2), a p type layer (InGaAs), and an intrinsic perovskite material that acts as an absorber from top to bottom.

The perovskite region is a location of creation of exitons (electron and bound state of a hole) when the solar cell is exposed to light. The collection mechanism of the photgenerated carriers is occured at ETL and HTL region. This phenomena is controlled by the carriers diffusion length and ETL (HTL) electrical properties. Exiton separation process happens at TiO2 / perovskite and perovskite/ InGaAs interfaces. The electrons migrate to the ETL (n) (TiO2) region, and the holes migrate to the HTL (p) (InGaAs) region. The mechanisms for dissociating and migrating are induced by the electric field between the TiO2/Perovskite and Perovskite/InGaAs.

Table 1 recapitulates the data inputs of the conventional and the proposed perovskite heterojunction solar cells. Real and imaginary refractive indices data are calculated from the SOPRA database [15]. We perform the simulation considering AM1.5 G solar spectrum.

Table 1
Physical model parameters assumed at T = 300 K.

Parameters	Designation	TiO_2 [16]	Perovskite [17]	InGaAs [18]
Eg (eV)	Band gap	3.2	1.55	0.75
ε	*permittivity*	19	100	13.88
τ_n *(S)*	Electron life time	10^{-7}	10^{-6}	1×10^{9}
τ_p *(S)*	Hole life time	10^{-7}	10^{-6}	1×10^{9}
υ_{sat} (cms^{-1})	carrier saturation velocity	-	-	1×10^{7}
χ *(eV)*	Affinity	4	3.8	4.5
N_c (cm^{-3})	Electron density of state	2×10^{18}	1×10^{19}	8.16×10^{16}
N_v (cm^{-3})	hole density of state	2×10^{19}	1×10^{17}	1×10^{18}

Here, E_g and ε_r represent the bandgap energy, and the material permittivity, respectively. τ_n and τ_p denote the carrier lifetimes, v_{sat} is the carrier saturation velocity, χ refers to the electron affinity, and N_c and N_v are the electron and hole density of states varying with temperature.

Iii. Physical Models

The ATLAS Silvaco simulator is used to model a heterojunction perovskite solar cell with InGaAs as the hole transport layer. To get the characteristics of the device during exposure to light, an advanced 3D LUMINOUS optoelectronic module is utilized. LUMINOUS determines the system's photo-generation by running two simultaneous simulations at each mesh point. LUMINOUS conducts an optical ray tracing inside the device via the refractive index n. The transmission and reflection rates of light are determined by changes in n values within layer boundaries. By tracking the light path from the origin to a mesh point, LUMINOUS can determine the optical intensity. The extinction coefficient k is used at each mesh position to quantify the absorption and photogeneration rates for the recorded optical intensity [19]. Most recombination mechanisms that can be classified as monomolecular, bimolecular, or trimolecular are taken into account in our modeling framework. Every one of those recombination processes is active at the same time, but the nature of the semiconductor favors one or more of them. Both organic and inorganic materials are modelled differently in the SILVACO ATLAS simulator. It is used in the current work with specific physical models, such as the Provskite organic case. The Pool–frenkel Field Model is particularly well suited to organic material mobility [20]. This should be calculated in conjunction with Langevin's recombination model. Recombination of Langevin is required to allow for the passage of charged carriers and single and triple excitons [21]. Just like TiO2 and InGaAs, the carrier concentration model is still applicable to inorganic materials [22].

Iv. Results And Discussions

1. Testing the simulation accuracy

It is important to note that the adopted simulation setup and model parameters are already supported by experimental results on ITO/TiO_2/$MAPbI_3$/Spiro-OMeTAD where good coincidence is achieved and the discrepancy may be attributed to the series resistance and the traps density [23].

Figure 2 shows the *J-V* characterestics and *QE* of the simulated ITO/TiO_2/$MAPbI_3$/Spiro-OMeTAD solar cell. An efficiency of 16.56% is acheived which is almost equal to that of the experimental one, however, a slight difference is remarked especially for V_{OC} and *FF* which is due principally to the interfacial traps effect and R_S and R_{SH} resistances.

2. The effect of InGaAs HTM candidate on the device optical and electrical performances

To reduce carrier recombination, the search for an effective inorganic HTM must be directed by the necessity for high carrier mobility, low cost, and a defect-free interface with the absorbing layer [24]. In

comparison to the spiro-OMeTAD, the inorganic p-type InGaAS, which has strong chemical stability, increased hole mobility, and a relatively inexpensive, is a perfect HTM [25]. In order to evade the blurred vision about the effectiveness of this HTM material in enhancing the solar cell performance a thorough investigation is performed.

Figure 3 depicts the band diagram of the proposed structure employing InGaAs as HTM. From this figure it is shown that the proposed HTM presents good electron bloking barrier which permit a reduced recombination at the interface perovskite/InGaAs.

Figure 4 shows the reflectance and transmittance of the suggested solar cell as function of wavelength. The reflectance at incoming wavelengths of 300 nm to 1000 nm is noticeably minimized at their specified wavelengths, as can be shown. The wavelengths where the coupling of thickness and refractive index permits destructive interference between the anti-phase reflected waves from the top and bottom interfaces correspond to the minimal reflectivity.

Figure 5 depicts the absorption coefficient as function of wavelength. It is clearly shown from this figure that the absorption attains high value at λ = 450nm, this can be linked to the band gap of the absorber layer which absorbs photons in this optical range.

A solar cell's quantum efficiency is known as the amount of the number of electrons generated in the external circuit by an incident photon of a specific wavelength. Consequently, external and internal quantum efficiencies (indicated by (*EQE*) and (*IQE*), respectively, can be defined. They vary in how photons reflected from the cell are treated: all photons intruding on the cell surface are included in the *EQE* value, and just photons that are not reflected are included in the *IQE* value.

The external quantum efficiency *EQE* determined from electrochemical measurements at a given wavelength is calculated using the following expression:

$$EQE = \frac{Isc}{Pin} \times \frac{hc}{e\lambda} \quad (1)$$

where *e* is the electron charge and hc/λ the photon energy. Uncertainties are rarely mentioned, but it seems difficult to determine EQE with an accuracy better than 3% [26]. The internal quantum efficiency (IQE) which is equal to EQE corrected for absorption and reflection losses, is expressed as follows:

$$IQE = \frac{EQE}{1-L} \quad (2)$$

Figure 6 illustrates the external and internal quantum efficiency variation across 300–1000 nm.

Although quantum efficiency should have the square form illustrated above, recombination effects limit quantum efficiency. Quantum efficiency is influenced by the same mechanisms that influence collection probability. Because blue light is absorbed extremely near to the surface, strong front surface recombination will impact the "blue" portion of the quantum efficiency. Green light is absorbed in the bulk of a solar cell, and a low diffusion length will decrease the quantum efficiency in the green section of the

spectrum by reducing the collection probability from the solar cell bulk. The quantum efficiency can be defined as the probability of collecting photons caused by a single wavelength's generation profile, multiplied by the device thickness and normalized to the incident quantity of photons.

3. Impact of In mole fraction variation

In order to elucidate the impact of InGaAs HTM with different molar fraction variation on the performance of the investigated solar cell an investigation is performed. It is noted that only gap, affinity and permittivity that are varied as function of In mole fraction. Figure 7 depicts the variation of the electrical outputs as function of different InGaAs mole fraction.

From this figure, it is clearly shown that the more the In content increase the more the V_{OC} increase, where V_{OC} increases from 0.7 V for x=0.1 to 1.18 V for x=0.8. This enhancement is not only due to the reduced $In_xGa_{1-x}As$ bandgap when compared to GaAs but also to the good perovskite/InGaAs interface engineering offset. As well, the J_{SC} and FF increase with increasing In mole fraction, this is attributed to the enhanced conductivity. The findings indicate that an In mole fraction of about 0.7 permits to reach high efficiency of 30%.

The J-V characteristics of the suggested solar cell are compared to the conventional solar cell in order to assess the influence of InGaAs HTM nominee on the solar cell electrical and optical performance. The acquired data are presented in Figure 8, where we can see that the suggested solar cell structure exhibits an obvious light absorption tendency that is superior to that of a conventional solar cell. This is mostly owing to the significant impact of the suggested construction using the InGaAs area on the solar cell's optical performance. It is noticed from this figure that the used InGaAs maintain the same V_{OC} as Spiro OMeTAD but also improves the J_{SC} by enhancing the carrier separation and collection mechanism through its high mobility and its narrow band gap which permit to cover wide range of light which augment the number of the photo-generated carriers.

Conclusion

In this study, Silvaco ATLAS is used to develop and evaluate a new p-InGaAs perovskite solar cell with a planar structure. The benefits of using InGaAs as HTM for perovskite heterojunction solar cell are investigated. The results reveal that the inclusion of InGaAs as HTM ,whith suitable In content, can influence the VOC, JSC and the FF. By assuring a high blocking layer and good collection mechanism the proposed structure can boost the efficiency to reach a high value (30%). The findings point to the possibility of creating a new perovskite cell structure that is both simpler and more efficient in the future.

Declarations

Conflict of interest

The authors declare that they have no known competing financial interests or personal relationships that could have appeared to influence the work reported in this paper.

References

1. Arpita Varadwaj, P.R., Varadwaj: Koichi Yamashita “Organic-Inorganic Hybrid CH3NH3PbI3 Perovskite Solar Cell Nanoclusters: Revealing Ultra-Strong Hydrogen Bonding and Mulliken Inner Complexes and Their Implication in Materials Design”. Chem. Mater. **28**, 4259 (2016). doi:10.1038/srep21687
2. Jiawei Gonga Jing Liangb K.Sumathy: “Review on dye-sensitized solar cells (DSSCs): Fundamental concepts and novel materials” Renewable and Sustainable Energy Reviews 5848-5860,October 2012, https://doi.org/10.1016/j.rser.2012.04.044
3. Mutalifu Abulikemu, J., Barbé, AbdulrahmanE., Labban, J., Eid, Silvano Del Gobbo “Planar heterojunction perovskite solar cell based on CdS electron transport layer” Journal of Thin Solid Films,512-518, 636, 31 August 2017, https://doi.org/10.1016/j.tsf.2017.07.003
4. Bendib, T., Bencherif, H., Abdi, M.A., Meddour, F., Dehimi, L., Chahdi, M.: Combined optical-electrical modeling of perovskite solar cell with an optimized design. Opt. Mater. **109**, 110259 (2020). doi:10.1016/j.optmat.2020.110259
5. Shariatinia, Z.. "Recent progress in development of diverse kinds of hole transport materials for the perovskite solar cells: A review," Renewable and Sustainable Energy Reviews, Elsevier, vol. 119(C)., 2020, DOI: 10.1016/j.rser.2019.109608
6. Ren, G., Han, W., Deng, Y., Wu, W., Li, Z., Guo, J.,a Bao, H.: Chunyu Liu and Wenbin Guo “Strategies of modifying spiro-OMeTAD materials for perovskite solar cells: a review” J. Mater.Chem.A,2021, https://doi.org/10.1039/D1TA05755C
7. Carlos Pereyra HaibingXie MónicaLira-Cantu: “Additive engineering for stable halide perovskite solar cells” Journal of Energy Chemistry, 599-634 September 2021, https://doi.org/10.1016/j.jechem.2021.01.037
8. Chaoqun Lu: Weijia Zhang *,Zhaoyi Jiang,Yulong Zhang andCong Ni “CuI/Spiro-OMeTAD Double-Layer Hole Transport Layer to Improve Photovoltaic Performance of Perovskite Solar Cells”. Coatings. **11**(8), 978 (2021). https://doi.org/10.3390/coatings11080978
9. Vinod, E., Madhavan, I., Zimmermann, A.A.B., Baloch, A., Manekkathodi, A., Belaidi: Nouar Tabet, and Mohammad Khaja Nazeeruddin “CuSCN as Hole Transport Material with 3D/2D Perovskite Solar Cells”. ACS Appl. Energy Mater. **3**(1), 114–121 (2020). https://doi.org/10.1021/acsaem.9b01692 ,9, 2019,
10. Lingyan, Lin,LinqinJiang,PingLi,BaodianF.Yu Qiu “A modeled perovskite solar cell structure with a Cu2O hole-transporting layer enabling over 20% efficiency by low-cost low-temperature processing” J. Phys. Chem. Solids,124, September 2018 DOI:10.1016/j.jpcs.2018.09.024
11. Li, S., Cao, Y.L., Li, W.H., et al.: A brief review of hole transporting materials commonly used in perovskite solar cells. Rare Met. **40**, 2712–2729 (2021). https://doi.org/10.1007/s12598-020-01691-

z

12. Zhiyong Liu, T., He, H., Wang, X., Song, H., Liu, J., Yang: Kaikai Liuc and Heng Mac “Improving the stability of the perovskite solar cells by V2O5 modified transport layer film”. RSC Adv. **7**, 18456–18465 (2017). DOI https://doi.org/10.1039/C7RA01303E
13. Babak Pashaei, S., Bellani: Hashem Shahroos and Francesco Bonaccorso “Molecularly engineered hole-transport material for low-cost perovskite solar cells”. Chem. Sci. **11**, 2429–2439 (2020). doi.org/10.1039/C9SC05694G
14. Lin, C.H., Sun, K.W., Liu, Q.M., Shirai, H., Lee, C.P.: “Poly(3,4ethylenedioxythiophene):poly(styrenesulfonate)/GaAs hybrid solar cells with 13% power conversion efficiency using front- and back-surface field” Opt. Express Vol. 23, Issue 19, pp. A1051-A1059 (2015) https://doi.org/10.1364/OE.23.0A1051
15. http://www.sspectra.com/sopra.html
16. BaoshunLiuaXiujianZhaoaJiaguoYubIvan, P.Parkinc,KazuyaNakata “Intrinsic intermediate gap states of TiO2 materials and their roles in charge carrier kinetics” Journal of Photochemistry and Photobiology C: Photochemistry Reviews,June 2019, https://doi.org/10.1016/j.jphotochemrev.2019.02.001
17. Samy Almosni,[b: c] Ludmila Cojocaru,[b] Debin Li,[d] Satoshi Uchida,*[a] Takaya Kubo, [b] and Hiroshi Segawa “Tunneling-Assisted Trapping as one of the Possible Mechanisms for the Origin of Hysteresis in Perovskite Solar Cells”. Energy Technol. **5**, 1767–1774 (2017). DOI:10.1002/ente.201700246
18. Guo-Qiang: HaoYong-gang, Zhang Yong-gang, Zhang Yi GuYi, Gu Show,Cheng Zhu “Performance analysis of extended wavelength InGaAs photovoltaic detectors grown with gas source MBE. ” JOURNAL OF INFRARED AND MILLIMETER WAVES (2006)
19. www.silvaco.com
20. Ganichev, S.D., Ziemann, E., Prettl, W., Yassievich, I.N., Istratov, A.A.: and E. R. Weber “Distinction between the Poole-Frenkel and tunneling models of electric-field-stimulated carrier emission from deep levels in semiconductors” Phys. Rev. B 61, 10361 – Published 15 April 2000 doi.org/10.1103/PhysRevB.61.10361
21. Timothy, M., Burke, S.S., Vandewal, K.:, and Michael D. McGehee “Beyond Langevin Recombination: How Equilibrium Between Free Carriers and Charge Transfer States Determines the Open-Circuit Voltage of Organic Solar Cells” Adv. Energy Mater. 1500123, 2015,DOI:10.1002/aenm.201500123
22. Lyu, M., Yun, J.H., Cai, M., et al.: Organic–inorganic bismuth (III)-based material: A lead-free, air-stable and solution-processable light-absorber beyond organolead perovskites. Nano Res. **9**, 692–702 (2016). https://doi.org/10.1007/s12274-015-0948-y
23. Qiu, W., Merckx, T., Jaysankar, M., Masse, C., de la Huerta, L., Rakocevic, W., Zhang, U.W., Paetzold, R., Gehlhaar, L., Froyen, J., Poortmans, D., Cheyns, H.J., Snaith, P.: Heremans “Pinhole-Free Perovskite Films for Efficient Solar Modules”. J. Name. **00**(3), 1 (2013). DOI:10.1039/x0xx00000x

24. Tejas, S., Sherkar, C., Momblona, L., Gil-Escrig, J., Ávila, M., Sessolo, H.J.. Bolink Orcid: and L. Jan Anton Koster Orcid “Recombination in Perovskite Solar Cells: Significance of Grain Boundaries, Interface Traps, and Defect Ions”. CS Energy Lett. **2**(5), 1214–1222 (2017). doi.org/10.1021/acsenergylett.7b00236
25. Jeon, N.J., Noh, J.H., Kim, Y.C., Yang, W.S., Ryu, S., Seok, S.I.: Solvent engineering for high-performance inorganic?organic hybrid perovskite solar cells. Nature Mater. **13**(9), 897–903 (2014). http://dx.doi.org/10.1038/nmat4014
26. Fischer, F.D., Simha, N.K., Predan, J., Schöngrundner, R.: & O. Kolednik On configurational forces at boundaries in fracture mechanics. Int. J. Fract. **174**, 61–74 (2012). https://doi.org/10.1007/s10704-011-9672-0

Figures

Figure 1

Schematic view of the conventional and proposed solar cells structures.

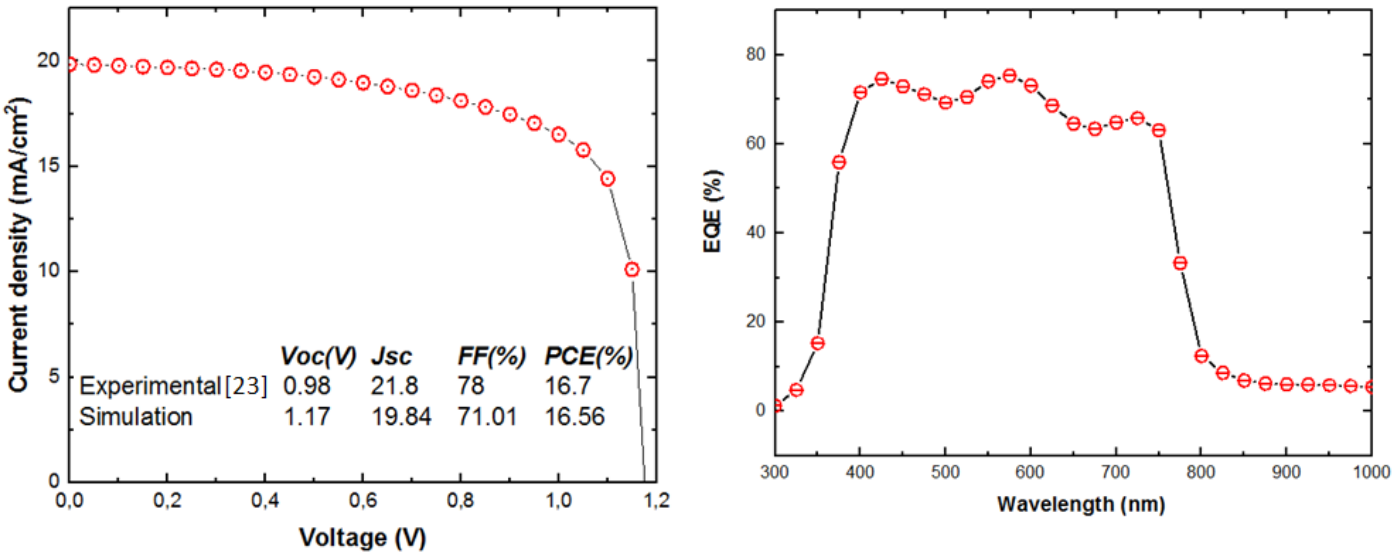

Figure 2

a) *J-V* characterestics b) *QE* of the simulated ITO/TiO2/MAPbI3/In0.7Ga0.3As/InAs Solar Cells

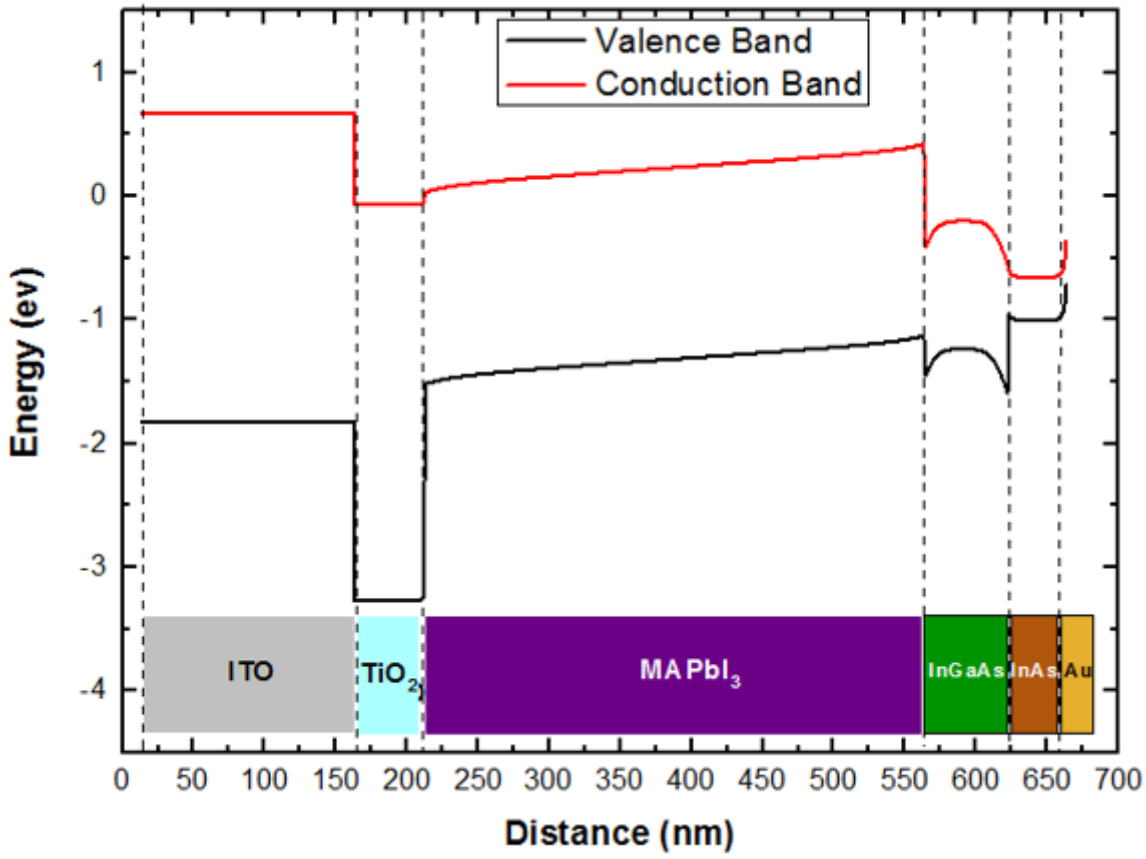

Figure 3

Band diagram of the proposed ITO/TiO_2/$MAPbI_3$/$In_{0.7}Ga_{0.3}As$/InAs Solar Cells

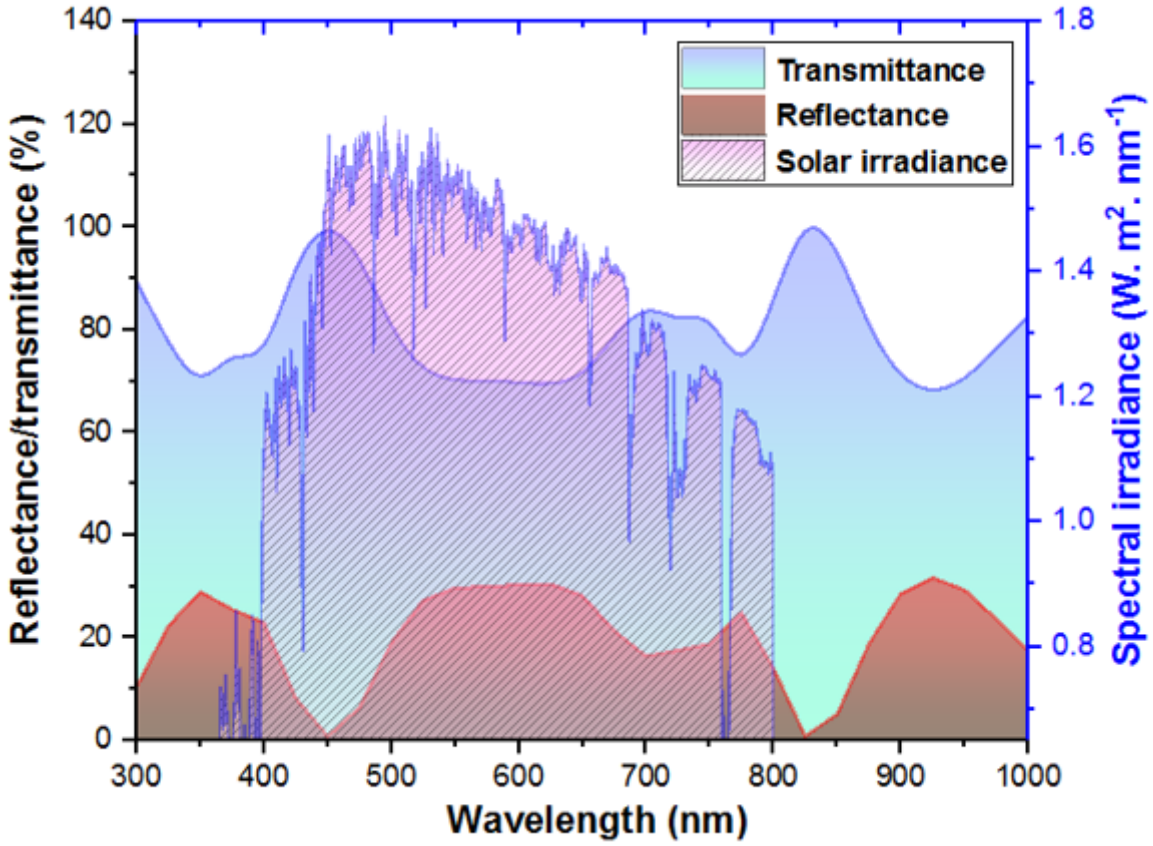

Figure 4

Reflectivity curves for the ITO/TiO2/MAPbI3/In0.7Ga0.3As/InAs Solar Cells.

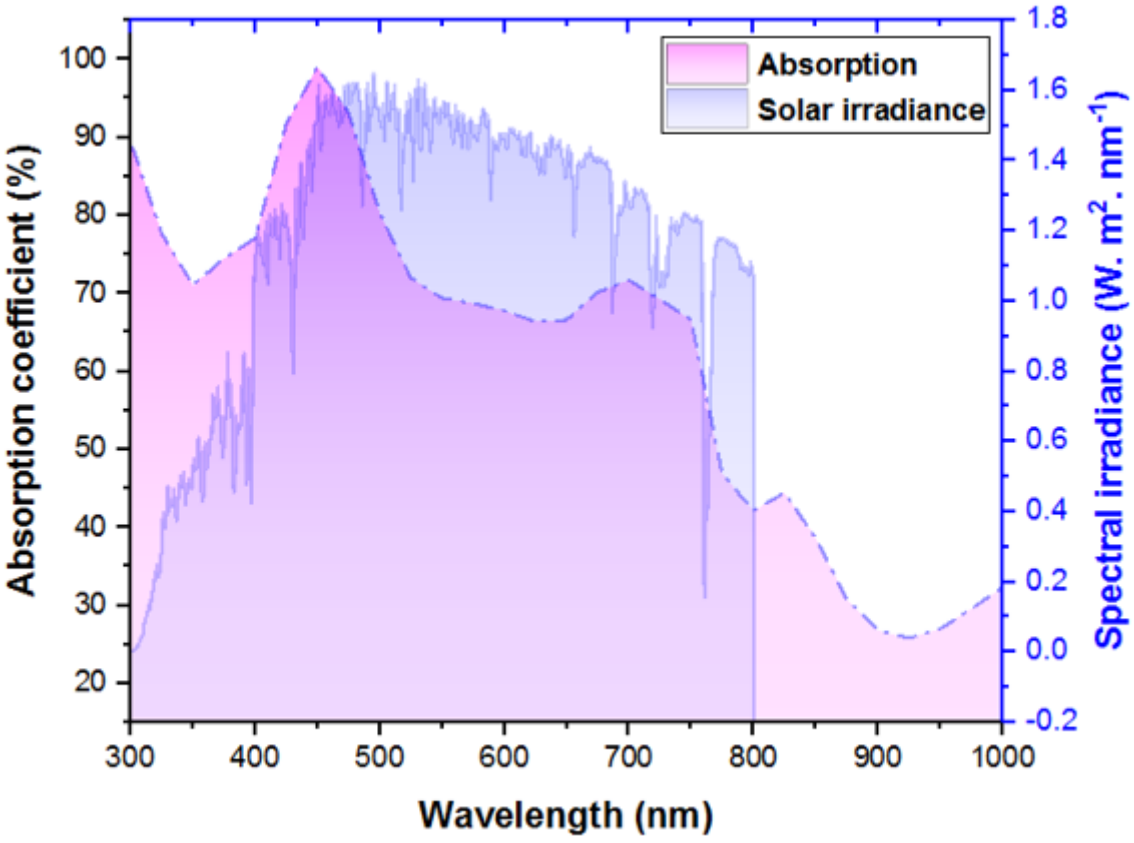

Figure 5

Absorption curves for the ITO/TiO_2/$MAPbI_3$/$In_{0.7}Ga_{0.3}As$/InAs Solar Cells

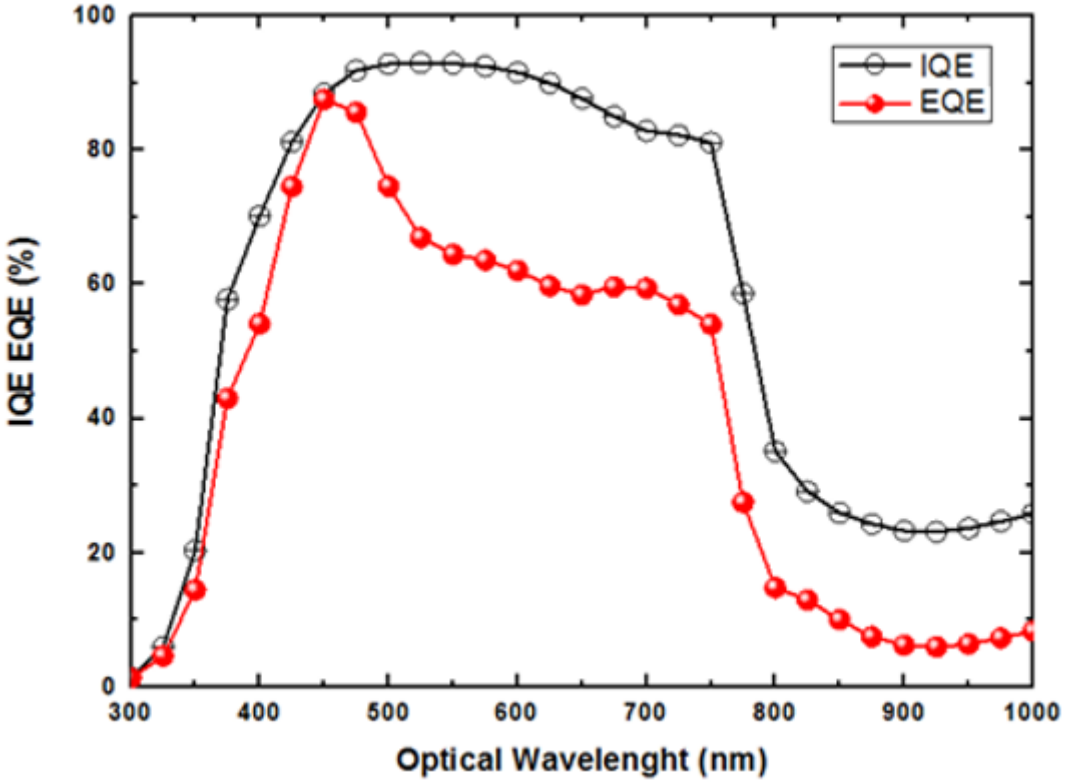

Figure 6

IQE and EQE curves of the investigated the ITO/TiO2/$MAPbI_3$/$In_{0.7}Ga_{0.3}As$/InAs Solar Cells.

Figure 7

Electrical outputs of the proposed solar cell as function of In mole fraction

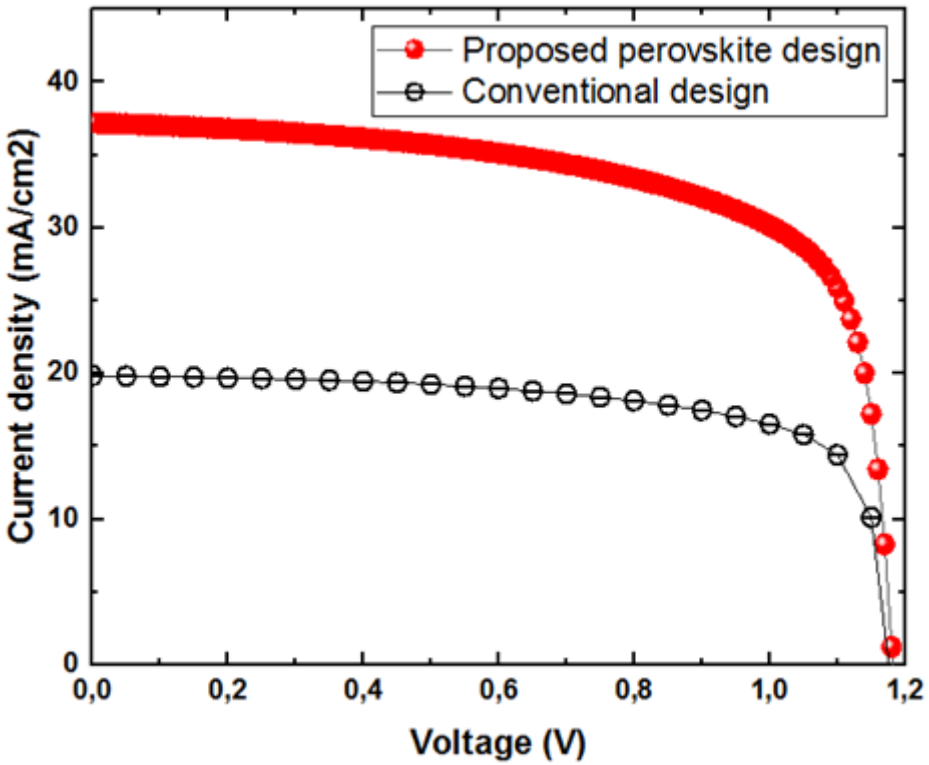

Figure 8

I-V curves for the ITO/TiO2/MAPbI3/In0.7Ga0.3As/InAs Solar Cells